Gas dynamic effects on formation of carbon dimers in laser-produced plasmas

K. F. Al-Shboul, S. S. Harilal,[a] and A. Hassanein
School of Nuclear Engineering and Center for Materials Under Extreme Environment, Purdue University, 400 Central Dr., West Lafayette, Indiana 47907, USA

(Received 31 August 2011; accepted 12 September 2011; published online 29 September 2011)

We investigated the effect of helium and nitrogen pressures on the dynamics of molecular species formation during laser ablation of carbon. For producing plasmas, planar carbon targets were irradiated with 1064 nm, 6 ns pulses from an Nd:yttrium aluminum garnet laser. The emission from excited C_2 and CN molecules was studied using space resolved optical time-of-flight emission spectroscopy and spectrally resolved fast imaging. The intensity oscillations in C_2 and CN monochromatic fast imaging and their emission space-time contours suggest that recombination is the major mechanism of C_2 formation within the laser ablation carbon plumes in the presence of ambient gas. © *2011 American Institute of Physics*. [doi:10.1063/1.3645631]

Because of numerous applications such as diamond-like carbon deposition and nanostructures synthesizing including nanotubes production, carbon laser-produced plasma (LPP) research was a main focus over the last several years.[1–4] In the context of carbon clusters and nanoparticles, it is believed that C_2 dimers play an important role in their formation.[2,5] Most commonly seen C_2 emission from these sources is the Swan band in the visible region of the spectra. While it was suggested that C_2 formation in the plasma within an ambient gas is comparable to the direct production from the target,[6–8] the formation mechanism of these clusters is still not clear[2,9] as where, when, and how these molecules form in the evolving carbon produced plasma. The dynamics of plasma plume expansion and the interaction with the ambient gas strongly affects the nature of cluster and nanoparticle production and laser deposition process, where the quality of the deposited films are strongly affected by the kinetic energy distributions of all plasma species.[3,10,11] Hence, more fundamental studies are essential to fully understand the mechanisms behind the formation of these nanostructures. Our recent measurements[12] indicate that C_2 emission zone in vacuum was just present near the target at early times. However, C_2 emission intensity was significantly enhanced near as well as far away from the target and the emission lifetime was extended in the presence of an ambient gas.

In this letter, the evolution of C_2 and CN species and their dynamics in carbon plasma have been investigated using spectrally resolved fast imaging and optical time-of-flight emission spectroscopy (OTOF-ES) to understand the formation mechanisms of C_2 and CN molecules in plasma plumes evolving in helium and nitrogen ambient gases. While C_2 can form, within the plasma, by recombination of carbon atoms and ions and dissociation of higher clusters, CN is mainly produced by recombination. A systematic comparison between C_2 and CN molecular species emission provides a better insight into their formation mechanisms in laser ablated plumes.

The experimental setup used in the present study is described elsewhere.[12] The plasma is generated by laser ablation of carbon targets using 1064 nm radiation pulses from Q-switched Nd:YAG laser with a repetition rate of 10 Hz and pulse width of 6 ns. The target in the form of a disc was mounted inside stainless steel vacuum chamber pumped down to a base pressure of about 10^{-6} Torr. The chamber was then filled with either helium or nitrogen gas at a certain pressure. The laser beam is focused normal to the target surface with 500 μm spot size and 50 Jcm^{-2} fluence. The plasma was imaged onto the slit of a 0.5 m spectrograph using appropriate collimating and focusing lenses. This optical system was translated to monitor different parts of the plume to obtain the OTOF-ES measurements by attaching the spectrograph to 1 ns rise time photomultiplier tube (PMT) for light detection. The 2-D plume imaging was accomplished by positioning an intensified charged-coupled device (ICCD) orthogonal to the plasma expansion direction. In order to discriminate C_2 and CN molecules from other species, narrow band-pass filters were used for filtering (0-0) C_2 Swan band transition at 516 nm and (0-0) CN Violet band transition at 388 nm.

The pathways of generating C_2 and CN excited molecules are different in LPP. As reported earlier[14] several formation mechanisms can lead for C_2 formation, while CN formation is mainly caused by recombination. The presence of CN is expected only in the presence of N_2 ambient while C_2 exists in all conditions including vacuum.[12] In order to differentiate C_2 and CN molecules in LPP, filtered fast imaging was accomplished in the presence of He and N_2 ambient at different pressure levels and is given in Figs. 1 and 2 along with spectrally integrated images. The gating time is incrementally increased (2-50 ns) to compensate the reduction in plasma intensity at later times. These images provide expansion dynamics as well as vital information about the plume species evolution after the onset of plasma. Each image given is obtained from a single laser shot and normalized to its maximum intensity for better clarity.

[a]Author to whom correspondence should be addressed. Electronic mail: sharilal@purdue.edu.

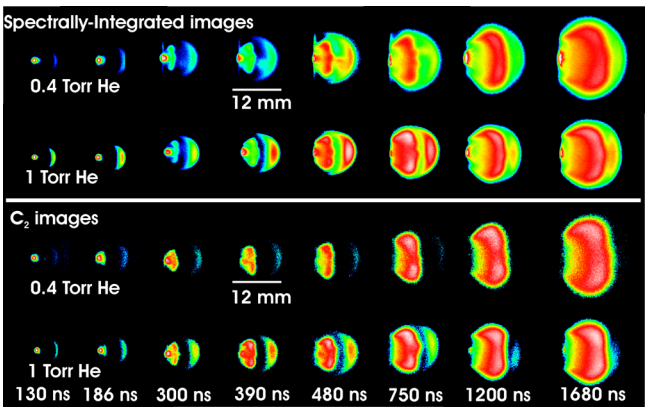

FIG. 1. (Color online) Spectrally integrated and C_2 monochromatic images of carbon plasma at 0.4 and 1 Torr He pressures. Each image is normalized to its maximum intensity.

As shown in Fig. 1, the ICCD images show enhanced emission from C_2 with increasing He pressure. At 0.4 Torr, the plume structure near to the target region (as seen in spectrally-integrated images) is similar to C_2 emission zone. However, C_2 emission is significantly weak in the plume front positions. On the other hand, at 1 Torr He pressure levels, the spatial distribution of C_2 emission is similar to the one obtained by the spectrally integrated images which implies that C_2 is the dominant emitting species in carbon plasma with increased He pressure. In all images, significant C_2 emission is noticed at the center of the plume and close to the target surface while enhanced emission from these species at plume front positions was evident only at higher He pressures. The enhanced emission from C_2 in the plume front positions with increasing pressure shows the role of recombination in the presence of He ambient.

Comparing C_2 and CN excited populations in the presence of N_2 ambient (Fig. 2) is helpful for understanding the gas dynamic effects. Because it is unclear from the images obtained in He ambient which mechanism is having major contribution for C_2 formation, we inserted N_2 ambient gas into the plasma chamber for generating CN molecules. Fig. 2 clearly shows that C_2 and CN population in LPP follows distinct spatial distributions. The CN molecules are evidently concentrated at the peripheries of the plume due to recombination and have significantly reduced emission in the plume center as well as closer to the target surface. It is clear from the spectrally integrated images that the carbon plasma is more confined in N_2 compared to He ambient that is due to heavier mass of nitrogen ambient in comparison with helium. It appears from the images (N_2, 1 Torr) that most of the emission in the stalled region is coming from excited C_2 formed due to recombination. The C_2 emission features in the N_2 ambient were similar to C_2 in He ambient except more confinement and enhanced emission at plume fronts.

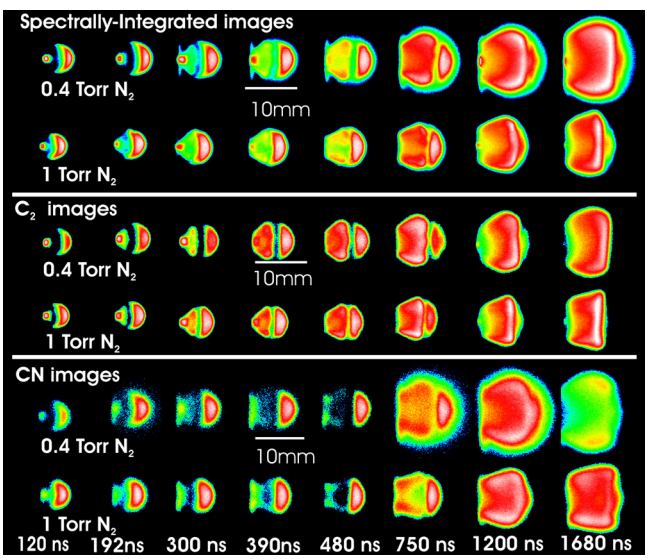

FIG. 2. (Color online) Spectrally integrated, CN monochromatic, and C_2 monochromatic images of carbon plasma at 0.4 and 1 Torr N_2 pressures.

In order to get a better insight of C_2 and CN expansion dynamics, OTOF-ES studies have been carried out. These studies provide critical information regarding the history of development of a certain excited species at a certain location in the plume after plasma formation with a time resolution better than 1 ns. Typical temporal distributions of C_2 ($\lambda = 516.5$ nm) and CN ($\lambda = 388.3$ nm) species obtained at 6 mm from the target are given in Fig. 3. The OTOF-ES profiles consist of a prompt peak at the earliest times followed by a sharp peak and finally a broad peak for both C_2 and CN.

Because of its highly dynamic behavior, LPP should be characterized in time and space resolved manner. Hence, space-time contours were generated from the OTOF-ES profiles in helium and nitrogen ambient at 0.4 and 1 Torr shown in Fig. 4 providing a comprehensive picture of the evolution history of C_2 and CN formation.

This multiple peak structures in the temporal evolution shows that both C_2 and CN have faster and slower components. The sharp peaks appeared at the earliest time in the OTOF-ES profiles are due to prompt electron excited ambient plasma and the details of this phenomena are given elsewhere.[13] Faster CN and C_2 peaks were observed immediately after the prompt peak. It is known that due to space charge effects, the highly charged ions in LPP possess the highest velocity and neutral species have the lowest velocity. The estimated expansion velocities for C and C^+ species under similar experimental conditions in vacuum are $2.9 \pm 0.1 \times 10^6$ cm/s and $4.6 \pm 0.1 \times 10^6$ cm/s respectively.[14] Our recorded velocities of the faster peaks for C_2 and CN at

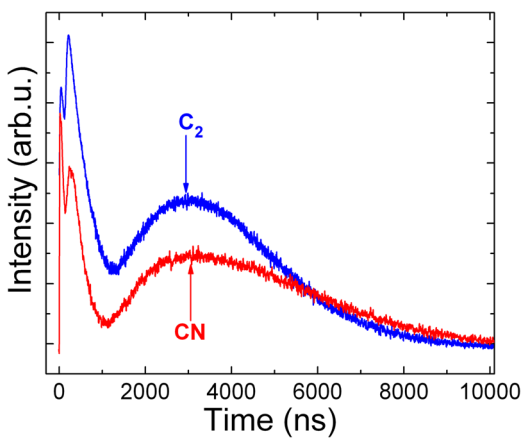

FIG. 3. (Color online) Typical OTOF-ES for C_2 ($\lambda = 516.5$ nm) and CN ($\lambda = 388.3$ nm) at 1 Torr N_2 ambient recorded at a distance 6 mm.

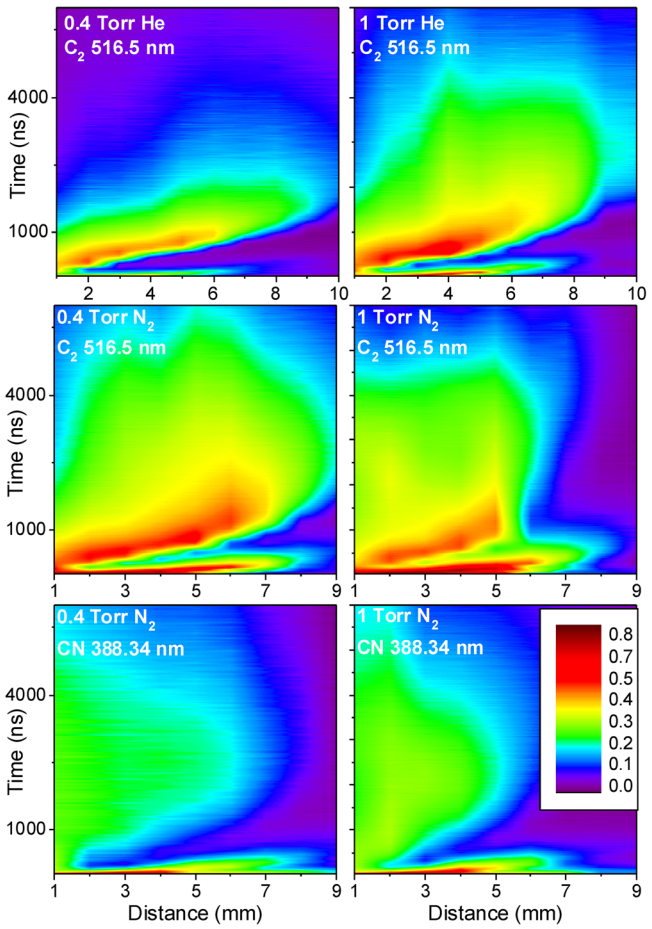

FIG. 4. (Color online) Space-time contours for both C_2 ($\lambda = 516.5$ nm) and CN ($\lambda = 388.3$ nm) in He and N_2 ambient at 0.4 and 1 Torr pressures.

1 Torr He are $1.2 \pm 0.1 \times 10^6$ cm/s and $1.0 \pm 0.1 \times 10^6$ cm/s. It should be mentioned that the plume propagation velocity will be reduced when it expands into an ambient because of plume-ambient species interaction. However, this interaction will be limited in the earliest times because of high plasma pressure. Hence the occurrence of C_2 and CN faster peaks, respectively, is due to recombination of carbon ions according to the following reactions:[15] $C^+ + C^+ + 2e^- \rightarrow C^* + C^* \rightarrow C_2^+ + e^- \rightarrow C_2^*$ and $2C^+ + 2e^- + N_2 \rightarrow 2CN^+ + 2e^- \rightarrow 2CN^*$, respectively.

It is interesting to note that these faster recombination peaks for C_2 and CN in OTOF-ES are found to be absent in fast images that leads us to believe that the dynamic range of the ICCD is not high enough to capture these photons. Though similar history is noticed for the faster peaks in the temporal profile of both CN and C_2 corresponding to ions recombination as discussed earlier, there are distinct dissimilarities in the delayed peaks. While CN molecules are obviously produced from recombination of carbon and nitrogen, there are two mechanisms behind the C_2 delayed formation peak. This C_2 peak could be a superposition of two contributing processes: dissociation of larger clusters and recombination of slow moving carbon neutrals[16] according to the following reaction:[15] $C^* + C^* \rightarrow C_2^+ + e^- \rightarrow C_2^*$. However, the agreement in the velocity ($\sim 6 \times 10^5$) from our TOF measurements for the broader delayed peaks of C_2 and CN in plume within ambient gas and with the velocity of the delayed peak of the slow moving neutrals indicates that the major mechanism for formation of delayed C_2 is due to recombination of slow moving excited neutrals while the long tail of C_2 delayed peak is due to dissociation of carbon clusters. Our previous results showed that the existence of C_2 in vacuum is limited to shorter distances and earliest times,[12] where an intense C_2 emission zone was noticeable near the focal spot in the monochromatic images even at late times which mainly can be attributed due to dissociation of clusters.

Fig. 4 clearly shows that the spatial extension of the C_2 is higher in the presence of He though its lifetime is increased in the presence of N_2 with a higher C_2 expansion velocity in He. These contours also show that increasing N_2 pressure from 0.4 to 1 Torr makes the delayed peak emission of C_2 weaker and decay faster. On the other hand, with increasing N_2 pressure, CN emission becomes more intense with enhanced decay times. It has been reported previously that[9,17] CN molecules can be formed on the basis of the following reaction: $C_2 + N_2 \rightarrow 2CN$, where C_2 is consumed for CN formation. This implies that C_2 is a precursor to CN production within carbon plasma in nitrogen ambient.

In conclusion, we investigated the C_2 and CN formation dynamics in carbon plasma in the presence of He and N_2 gases. A combination of two diagnostic methods, i.e., filtered fast imaging and OTOF-ES, provided better insights about these species development history and formation mechanisms. Our results showed that C_2 formation in laser plumes within ambient gas is due to recombination through fast moving ions, slow moving neutrals in addition to cluster dissociation. The comparison between C_2 and CN filtered fast imaging and space-time emission contours in ambient gases leads us to conclude that recombination is the major mechanism for the formation of C_2 species in laser ablation plumes.

This work was supported US DOE NNSA under Award number DE-NA0000463.

[1]D. B. Geohegan, H. Schittenhelm, X. Fan, S. J. Pennycook, A. A. Puretzky, M. A. Guillorn, D. A. Blom, and D. C. Joy, Appl. Phys. Lett. **78**, 3307 (2001).
[2]M. K. Moodley and N. J. Coville, Chem. Phys. Lett. **498**, 140 (2010).
[3]J. Seth, R. Padiyath, and S. V. Babu, Appl. Phys. Lett. **63**, 126 (1993).
[4]J. J. Camacho, L. Diíaz, M. Santos, L. J. Juan, and J. M. L. Poyato, J. Appl. Phys. **106**, 033306 (2009).
[5]D. M. Gruen, S. Liu, A. R. Krauss, J. Luo, and X. Pan, Appl. Phys. Lett. **64**, 1502 (1994).
[6]C. Lifshitz, Int. J. Mass Spectrom. **200**, 423 (2000).
[7]E. A. Rohlfing, D. M. Cox, and A. Kaldor, J. Chem. Phys. **81**, 3322 (1984).
[8]K. Sasaki, T. Wakasaki, S. Matsui, and K. Kadota, J. Appl. Phys. **91**, 4033 (2002).
[9]G. M. Fuge, M. N. R. Ashfold, and S. J. Henley, J. Appl. Phys. **99**, 014309 (2006).
[10]C. Aruta, S. Amoruso, R. Bruzzese, X. Wang, D. Maccariello, F. Miletto Granozio, and U. Scotti di Uccio, Appl. Phys. Lett. **97**, 252105 (2010).
[11]D. Riabinina, M. Chaker, and F. Rosei, Appl. Phys. Lett. **89**, 131501 (2006).
[12]K. F. Al-Shboul, S. S. Harilal, A. Hassanein, and M. Polek, J. Appl. Phys. **109**, 053302 (2011).
[13]S. S. Harilal, B. O'Shay, Y. Tao, and M. S. Tillack, J. Appl. Phys. **99**, 083303 (2006).
[14]S. S. Harilal, A. Hassanein, and M. Polek, J. Appl. Phys. **110**, 053301 (2011).
[15]C. Park, J. T. Howe, R. L. Jaffe, and G. V. Candler, J. Thermophys. Heat Transfer **8**, 9 (1994).
[16]Y. Iida and E. S. Yeung, Appl. Spectrosc. **48**, 945 (1994).
[17]H. S. Park, S. H. Nam, and S. M. Park, J. Appl. Phys. **97**, 113103 (2005).